

See discussions, stats, and author profiles for this publication at: <https://www.researchgate.net/publication/44650611>

# Change of the Binding Mode of the DNA/Proflavine System Induced by Ethanol

ARTICLE in THE JOURNAL OF PHYSICAL CHEMISTRY B · JULY 2010

Impact Factor: 3.3 · DOI: 10.1021/jp102801z · Source: PubMed

---

CITATIONS

22

---

READS

21

6 AUTHORS, INCLUDING:



**Begoña García**

Universidad de Burgos

155 PUBLICATIONS 1,532 CITATIONS

SEE PROFILE



**Rebeca Ruiz**

Complutense University of Madrid

12 PUBLICATIONS 179 CITATIONS

SEE PROFILE



**Tarita Biver**

Università di Pisa

70 PUBLICATIONS 657 CITATIONS

SEE PROFILE

## Change of the Binding Mode of the DNA/Proflavine System Induced by Ethanol

Begoña García,<sup>\*,†</sup> José M. Leal,<sup>†</sup> Rebeca Ruiz,<sup>†</sup> Tarita Biver,<sup>‡</sup> Fernando Secco,<sup>\*,‡</sup> and M. Venturini<sup>‡</sup>

Chemistry Department, University of Burgos, 09001 Burgos, Spain, and Chemistry and Industrial Chemistry Department, University of Pisa, 56126 Pisa, Italy

Received: March 29, 2010; Revised Manuscript Received: May 14, 2010

The equilibria and kinetics of the binding of proflavine to poly(dG-dC)•poly(dG-dC) and poly(dA-dT)•poly(dA-dT) were investigated in ethanol/water mixtures using spectrophotometric, circular dichroism, viscometric, and *T*-jump methods. All methods concur in showing that two modes of interaction are operative: intercalation and surface binding. The latter mode is favored by increasing ethanol and/or the proflavine content. Both static and kinetic experiments show that, concerning the poly(dG-dC)•poly(dG-dC)/proflavine system, intercalation largely prevails up to 20% EtOH. For higher EtOH levels surface binding becomes dominant. Concerning the poly(dA-dT)•poly(dA-dT)/proflavine system, melting experiments show that addition of proflavine stabilizes the double stranded structure, but the effect is reduced in the presence of EtOH. The  $\Delta H^\circ$  and  $\Delta S^\circ$  values of the melting process, measured at different concentrations of added proflavine, are linearly correlated, revealing the presence of the enthalpy–entropy compensation phenomenon (EEC). The nonmonotonicity of the “entropic term” of the EEC reveals the transition between the two binding modes. *T*-jump experiments show two relaxation effects, but at the highest levels of EtOH (>25%) the kinetic curves become monophasic, confirming the prevalence of the surface complex. A branched mechanism is proposed where diffusion controlled formation of a precursor complex occurs in the early stage of the binding process. This evolves toward the surface and/or the intercalated complex according to two rate-determining parallel steps. CD spectra suggest that, in the surface complex, proflavine is bound to DNA in the form of an aggregate.

## Introduction

The process whereby drugs and mutagens possessing planar aromatic rings interact with double/triple-stranded nucleic acids has been the subject of extensive studies, following the original hypothesis of the intercalation model proposed by Lerman<sup>1</sup> as a result of the interpretation of roentgenograms and viscometric experiments on the DNA/proflavine system. The Lerman hypothesis has become so popular that the majority of the results about the binding of planar drugs to nucleic acids are interpreted according to this mode of interaction, although information provided by accurate pioneer studies showed that intercalation is not a straightforward process. A diligent analysis of spectrophotometric data concerning the binding of proflavine to DNA demonstrated the formation of two bound forms, originally denoted as “weak” and “strong” complexes.<sup>2</sup> This initial observation was corroborated by the results of early kinetic experiments on the same system, which showed the occurrence of two<sup>3</sup> or even three<sup>4</sup> relaxation effects. In subsequent investigations a single relaxation effect was recorded,<sup>5,6</sup> but all of these studies concurred in demonstrating the biphasic nature of the process. However, some variations in the reaction parameter values, such for example the site size dependence on the concentration of added salt<sup>7</sup> or rate dependence on base pair nature (AT vs GC)<sup>8</sup> make any conclusion about the mechanism of dye binding to DNA rather uncertain. The complexity of the system makes it difficult to separate the contributions of the forces that are at work during the DNA–drug interaction.

These forces are of electrostatic and nonelectrostatic (stacking) nature and both can play a fundamental role in the nucleic acid chemistry and in the solution chemistry of the dyes. In spite of the many efforts made to enlighten this issue, the various contributions of these forces to the overall free energy change of the binding process remain difficult to analyze.<sup>9</sup> The importance of changing the properties of the solvent, to investigate the origin of the electrostatic and stacking interactions, is well recognized. In this context, alcohols are known to remarkably affect the strength of electrostatic forces and to weaken hydrophobic effects.<sup>10,11</sup> The perturbation of the aqueous solvent by means of alcohols does constitute, therefore, a useful tool to elucidate the role of electrostatic and hydrophobic forces on the DNA–drug interaction.

With the present work we have tried to shed light into the nature of the interaction that accompanies the binding of proflavine to poly(dA-dT)•poly(dA-dT) and poly(dG-dC)•poly(dG-dC), looking in particular to the influence exerted on the binding modes by the base-pair nature and the solvent, using water–ethanol mixtures. The static studies have been performed by employing a variety of techniques such as spectrophotometry, circular dichroism, and viscosity, while the kinetic investigation has been carried out using the *T*-jump relaxation technique.

## Experimental Section

**Materials.** Calf thymus DNA (CT-DNA) and the synthetic polynucleotides poly(dA-dT)•poly(dA-dT) and poly(dG-dC)•poly(dG-dC) were purchased from Sigma-Aldrich as the lyophilized sodium salts and used without further purification. The CT-DNA was sonicated as described below. Stock solutions of the polynucleotides were standardized spectrophotometrically

\* Corresponding authors. E-mail: B.G., begar@ubu.es; F.S., ferdi@cci.unipi.it.

<sup>†</sup> University of Burgos.

<sup>‡</sup> University of Pisa.

using  $\varepsilon = 1.32 \times 10^4 \text{ M}^{-1} \text{ cm}^{-1}$  ( $\lambda = 260 \text{ nm}$ ) for CT-DNA,<sup>12</sup>  $\varepsilon = 1.33 \times 10^4 \text{ M}^{-1} \text{ cm}^{-1}$  ( $\lambda = 260 \text{ nm}$ ) for poly(dA-dT)•poly(dA-dT),<sup>13</sup> and  $\varepsilon = 1.68 \times 10^4 \text{ M}^{-1} \text{ cm}^{-1}$  ( $\lambda = 254 \text{ nm}$ ) for poly(dG-dC)•poly(dG-dC).<sup>14</sup> The polynucleotide concentrations employed in this work are expressed in molarity of base pairs and are indicated as  $C_p$ .

Proflavine (PR) hydrochloride of analytical grade from Sigma was used without further purification. The stock solutions were standardized by absorbance measurements at 444 nm, using  $\varepsilon = 4.2 \times 10^4 \text{ M}^{-1} \text{ cm}^{-1}$ <sup>15</sup> and kept in the dark at 4 °C. The molar concentration of proflavine has been denoted as  $C_D$ .

Sodium chloride was used to adjust the ionic strength, and sodium cacodylate,  $2.5 \times 10^{-3} \text{ M}$ , was employed to keep the solutions at pH 7.0.

Doubly distilled water from a Millipore Q apparatus was used to prepare the solutions and as a reaction medium. All solutions were prepared frequently and kept in the dark.

**Methods.** Measurements of pH were performed using a Metrohm 16 DMS Titrino pH-meter fit out with a combined glass electrode with a 3 M KCl solution as a liquid junction.

DNA was sonicated with a MSE-Sonyprep sonicator, by applying to suitable CT-DNA samples (10 mL of CT-DNA ca.  $2 \times 10^{-3} \text{ M}$ ) seven repeated cycles of 10 s sonication and 20 s pause, at an amplitude of 14  $\mu\text{m}$ . The sonicator tip was introduced directly into a solution kept in an ice bath to minimize the thermal effects. Agarose gel electrophoresis tests indicated that the polymer length was reduced to ca. 800 base-pairs. Thermal denaturation studies and spectrophotometric titrations were performed on a Hewlett-Packard 8453A spectrophotometer (Agilent Technologies, Palo Alto, CA) fit out with photodiode array detection and computer-assisted temperature control systems ( $\pm 0.1$  °C). Thermal denaturation experiments of the poly(dA-dT)•poly(dA-dT)/PR system were carried out in different ethanol/water media, using  $C_p = 1.5 \times 10^{-5} \text{ M}$  and varying the  $C_D/C_p$  ratio from 0 to 2. On the other hand, the melting temperature of systems containing poly(dG-dC)•poly(dG-dC) could not be determined because of the high melting temperature.<sup>16</sup> The titrations were carried out by adding increasing amounts of the polynucleotide directly into the cell containing the drug solution, whose concentration was  $4.6 \times 10^{-6} \text{ M}$ . Binding measurements have been performed at 25 °C and pH 7.0, whereas two different ionic strength values, 0.0025 or 0.1 M, were used. Data were analyzed at  $\lambda = 430 \text{ nm}$ , where only free and bound proflavine absorb.

Circular dichroism (CD) spectra were recorded on a MOS-450 Bio-Logic spectrophotometer (Claix, France). Quartz cells of 1.0 cm path length have been used. The CD titrations have been carried out adding increasing amounts of proflavine into the cell containing the polynucleotide solution,  $C_p = 5.5 \times 10^{-5} \text{ M}$ , varying the  $C_D/C_p$  ratio from 0 to 2.

Viscosity measurements were performed using a Micro-Ubbelohde viscometer whose temperature was controlled by an external thermostat ( $25 \pm 0.1$  °C). The viscosity data were analyzed using eq 1, where  $t_0$  and  $t_{\text{DNA}}$  are the flow times of the solvent and DNA solution, respectively, while  $t$  is the flow time of the proflavine and DNA mixture. Mean values of replicated measurements were used to evaluate the viscosity of the sample,  $\eta$ , and that of DNA alone,  $\eta_0$ .<sup>17</sup>

$$\eta/\eta_0 = (t - t_0)/(t_{\text{DNA}} - t_0) \quad (1)$$

Chemical relaxation experiments were performed on a Joule heating  $T$ -jump instrument described in a previous work,<sup>18</sup> using the fluorescence detection mode. The signal revealing the course

of the reaction was recorded by a Tektronix 2212 digital oscilloscope and transferred to a personal computer via a GPIB interface and analyzed by a nonlinear least-squares procedure specifically devised to fit multiexponential functions.<sup>19</sup> The relaxation time values used in the data analysis were averaged over at least six repeated experiments with a maximum spread of 10%. The temperature of the solutions was controlled to within  $\pm 0.1$  °C.

## Results

**Equilibria.** Proflavine (denoted as PR and, occasionally, as dye or drug) dissolved in water is known to undergo dimerization in aqueous solution at concentrations higher than  $3 \times 10^{-5} \text{ M}$ .<sup>20,21</sup> On the other hand, it is known that the extent of the self-aggregation process of this drug is reduced in water/EtOH mixtures.<sup>22</sup> To avoid complications due to coupling of such a reaction with the drug binding to DNA, the possibility that proflavine could self-aggregate in the water/EtOH mixtures was explored. Figure S1 of the Supporting Information shows that the absorbance dependence on drug concentration is linear, thus assuring the absence of free drug aggregation under the conditions of the binding equilibrium measurements. This feature does not exclude drug aggregation on the DNA surface (see below).

The binding of proflavine to DNA can be represented by the apparent reaction (2)



where D and PD denote the free and bound dye, respectively, whereas P indicates the polymer free sites.

Figure 1 shows the spectral changes of the two investigated systems, recorded during titrations performed at different EtOH contents. The lack of isosbestic points observed for poly(dA-dT)•poly(dA-dT)/PR system in 0% EtOH suggests that, under these circumstances the binding process is not a simple one. In contrast, in 30% EtOH the system displays a well-defined isosbestic point. The poly(dG-dC)•poly(dG-dC)/PR system shows a single isosbestic point at 457 nm in 0% EtOH, which is displaced to 463 nm in 30% EtOH, suggesting that in each medium only one complex is prevailing.

The titration data have been processed according to eq 3.

$$C_D/\Delta A = 1/\Delta\varepsilon + 1/(K\Delta\varepsilon[P]) \quad (3)$$

The variable  $\Delta A = A - A_D$ , where  $A_D$  is the absorbance of the dye in the absence of DNA, stands for the change of absorbance, while the parameter  $\Delta\varepsilon = \varepsilon_{PD} - \varepsilon_D$  is the extinction coefficient difference between PD and D. The concentration of the bound dye is experimentally determined as  $[PD] = \Delta A/\Delta\varepsilon$  and the free site concentration,  $[P]$ , has been evaluated according to the relationship  $[P] = C_p f(r)$ , where  $r = [PD]/C_p$  and  $f(r) = (1 - nr)^n / (1 - (n - 1)r)^{n-1}$ .<sup>23,24</sup> The site size,  $n$ , of the system has been determined from titrations at very low ionic strength ( $I = 0.0025 \text{ M}$ ), where the binding reaction evolves to completion. The evaluation of  $n$  is shown in Figure S2 of the Supporting Information, while the values obtained, between 0 and 30% EtOH, are reported in Table 1. Both systems show a remarkable increase of  $n$  as the ethanol percentage increases.

Binding isotherms of two typical titrations are shown in Figure 2, while in Figure S3 of the Supporting Information

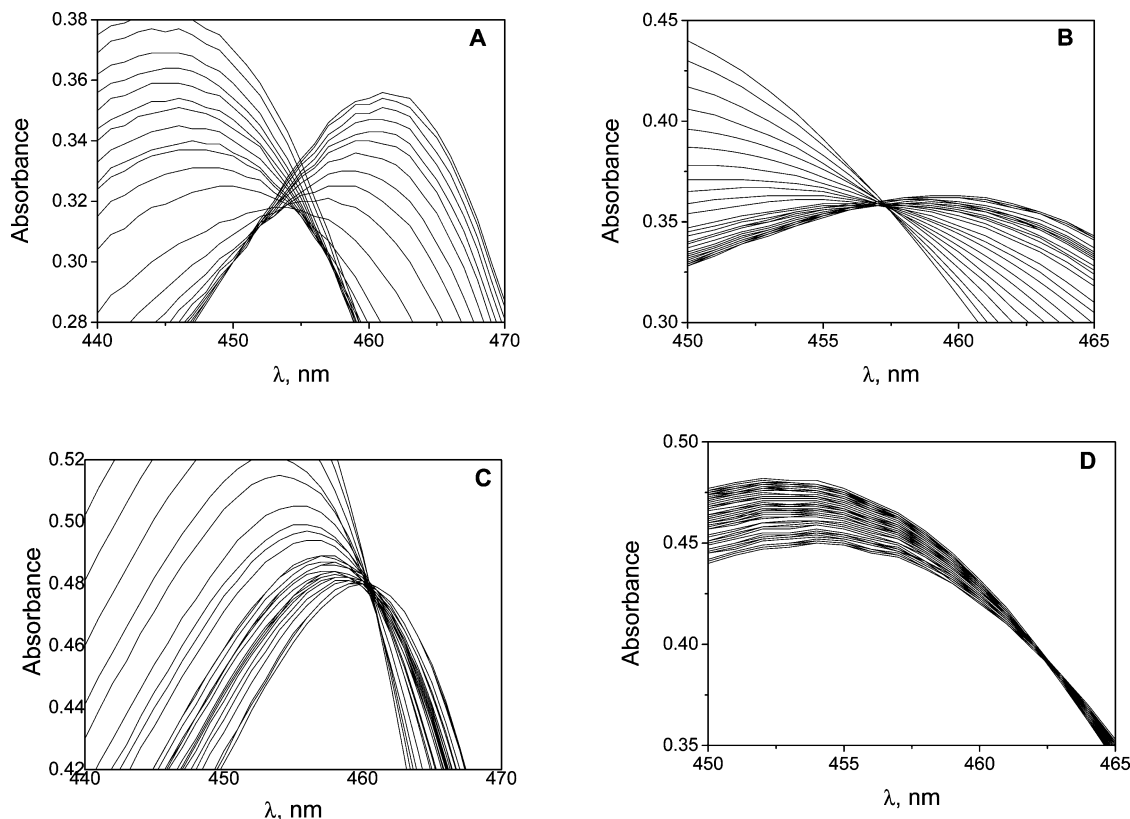


**Figure 1.** Spectral changes of the DNA/PR systems recorded during titrations.  $C_D = 1.10 \times 10^{-5}$  M,  $I = 0.1$  M (NaCl), pH = 7.0,  $T = 25$  °C. Poly(dA-dT)·poly(dA-dT)/PR: (A) 0% EtOH; (B) 30% EtOH. Poly(dG-dC)·poly(dG-dC)/PR: (C) 0% EtOH; (D) 30% EtOH.

**TABLE 1: Binding Constants of the Poly(dA-dT)·poly(dA-dT)/PR and Poly(dG-dC)·poly(dG-dC)/PR Systems ( $I = 0.1$  M) and  $n$  Values ( $I = 0.0025$  M) in Different Percent EtOH, pH = 7.0,  $T = 25$  °C**

% EtOH	poly(dA-dT)·poly(dA-dT)/PR		poly(dG-dC)·poly(dG-dC)/PR	
	$n$	$10^{-4}K, \text{M}^{-1}$	$n$	$10^{-4}K, \text{M}^{-1}$
0	1.2	$7.2 \pm 0.1$	1.4	$6.1 \pm 0.2$
5	1.7	$13.2 \pm 0.4$	1.7	$10.3 \pm 0.1$
10	2.1	$18.7 \pm 0.2$	1.9	$5.0 \pm 0.1$
15	2.4	$9.5 \pm 0.2$	2.3	$3.9 \pm 0.1$
20	2.8	$4.0 \pm 0.5$	2.7	$1.0 \pm 0.1$
25	3.1	$4.1 \pm 0.3$	3.0	$0.86 \pm 0.02$
30	3.5	$1.9 \pm 0.2$	4.8	

analysis according to eq 3 is shown. The values of the binding constant,  $K$ , are collected in Table 1. Concerning poly(dG-dC)·poly(dG-dC)/PR in 30% of ethanol, absorbance changes were so small that analysis of the data could not provide reliable results.

**Melting Experiments.** The melting process of poly(dA-dT)·poly(dA-dT) was monitored by spectrophotometry. The single strand fraction,  $\alpha$ , has been evaluated using eq 4

$$\alpha = (A - A_D)/(A_S - A_D) \quad (4)$$

where  $A_D$ ,  $A_S$ , and  $A$  stand for the absorbance of the double strand, single strand, and mixture, respectively. Figure 3 shows a plot of  $da/dT$  vs  $T$  corresponding to the melting curve in 10% EtOH. One can observe that the maximum (associated to the melting temperature,  $T_m$ ) moves toward higher temperatures as the proflavine content is increased, while the amplitude of the curves, which measures the hyperchromism of the system,

decreases. The increase of  $T_m$  with  $C_D/C_P$ , which has been associated with drug intercalation,<sup>25</sup> becomes less and less pronounced as the % EtOH is raised (Figure 4).

Considering the melting process as a dissociation of the double helix into single strands, the denaturation constant,  $K_d$ , is expressed by eq 5

$$K_d = 4C_P\alpha^2/(1 - \alpha) \quad (5)$$

Considering the data in the vicinity of the melting point,<sup>26</sup> plots of  $\ln K_d$  vs  $1/T$  are linear (Figure S4 of the Supporting Information) and allow us to obtain the values of  $\Delta H^\circ_{vH}$  and  $\Delta S^\circ_{vH}$  for the melting process that are collected in Table 2.

To assess the validity of the values of the melting temperature and van't Hoff melting enthalpies obtained by spectrophotometric method and given in Table 2, the values of  $T_m$  and  $\Delta H^\circ_{vH}$  have been determined also by a differential scanning calorimetry experiment (Figure S5 of the Supporting Information) performed in 0% EtOH and for  $C_D/C_P = 0$ . The results obtained,  $T_m = 61.2$  °C and  $\Delta H^\circ_{vH} = 330$  kcal mol<sup>-1</sup>, are in pretty good agreement with the optical determination. Moreover, integration of the calorimetric curve provides the value of  $\Delta H^\circ_{cal}$  (10 kcal mol<sup>-1</sup>), which represents the enthalpy variation associated to the double-strand dissociation independently of the model adopted. The noncoincidence of the  $\Delta H^\circ_{vH}$  and  $\Delta H^\circ_{cal}$  has been ascribed to the cooperativity of the melting process, which is fundamentally different from the model to which the van't Hoff argument has been applied to evaluate  $\Delta H^\circ_{vH}$ .<sup>27</sup>

**Enthalpy–Entropy Compensation.** The values of  $\Delta H_{vH}$ , obtained for different values of the  $C_D/C_P$  ratio, have been plotted vs the corresponding values of  $\Delta S_{vH}$  for each of the five investigated EtOH/H<sub>2</sub>O compositions. All plots are linear (see



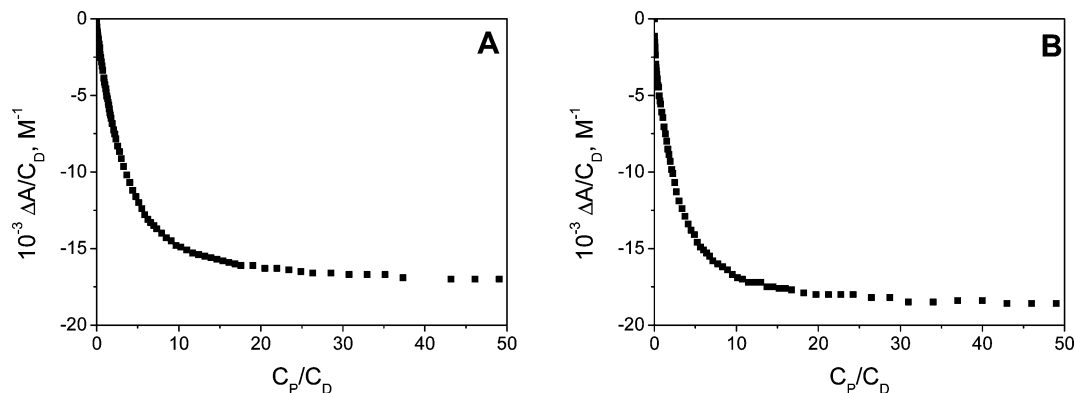


**Figure 2.** Binding isotherms for the poly(dA-dT)·poly(dA-dT)/PR (A) and poly(dG-dC)·poly(dG-dC)/PR (B) systems in 5% EtOH.  $I = 0.1$  M (NaCl), pH = 7.0,  $T = 25$  °C,  $\lambda = 430$  nm.

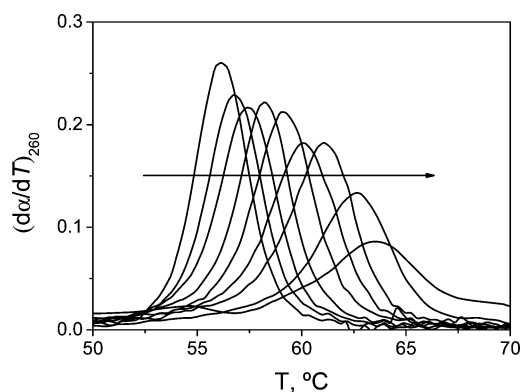


**Figure 3.** Plot of  $d\alpha/dT$  vs  $T$  for the poly(dA-dT)·poly(dA-dT)/PR system in 10% EtOH.  $C_P = 1.5 \times 10^{-5}$  M,  $C_D/C_P$  = from 0 to 1.92 (arrow's sense).  $I = 0.1$  M (NaCl), pH = 7.0,  $\lambda = 260$  nm.

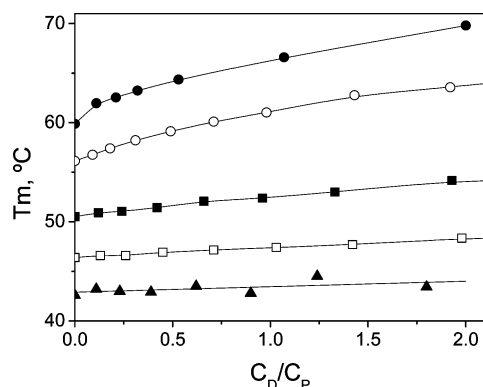


**Figure 4.** Melting temperature of the poly(dA-dT)·poly(dA-dT)/PR system as a function of  $C_D/C_P$  for different ethanol/water mixtures: (●) 0, (○) 10, (■) 20, (□) 30 y (▲) 40% EtOH.  $I = 0.1$  M (NaCl), pH = 7.0.

Figure S6 of the Supporting Information as an example) in agreement with the relationship

$$H = aS + b \quad (6)$$

which is applicable when there is a linear enthalpy–entropy interdependence. Equation 6 constitutes the basis of the general thermodynamic model proposed by Starikov and Nordén<sup>28</sup> to interpret valid enthalpy–entropy compensation phenomena. There,  $H$  and  $S$  are enthalpy and entropy, respectively,  $a$  is the so-called “compensation temperature”, and  $b$  has the dimension of energy. The parameters of eq 6 obtained from plots as that of Figure S6 are reported in Table 3 for each solvent composition. The table shows that the “entropic term”, i.e., the  $a/b$  ratio

is clearly nonmonotonic, exhibiting a maximum at 20% EtOH. Also, the compensation temperature,  $a$ , displays its minimum value while the parameter  $b$  displays a maximum value.

**Circular Dichroism Measurements.** Addition of proflavine to poly(dA-dT)·poly(dA-dT) and poly(dG-dC)·poly(dG-dC) gives rise to perturbations of the CD spectra in the UV region and to formation of new bands in the visible range (induced circular dichroism). Figure 5 shows the CD spectra of the two studied systems in 0%, 10%, and 30% EtOH. The influences of proflavine on the visible CD bands of poly(dA-dT)·poly(dA-dT) and poly(dG-dC)·poly(dG-dC) are quite similar. However, addition of PR to the solutions containing 30% EtOH affects the UV bands of poly(dA-dT)·poly(dA-dT) to a much larger extent.

**Poly(dA-dT)·poly(dA-dT)/PR.** The UV–CD spectra of poly(dA-dT)·poly(dA-dT) in the absence of ethanol (Figure 5A) show that both the negative and positive bands do increase as the  $C_D/C_P$  ratio does, exhibiting an isoelliptic point at 255 nm located in the positive region. As the ethanol content is raised, the spectral sequence displays a remarkable change. Already in 10% EtOH it is possible to observe the disruption of the isoelliptic point, while a new family of spectra start to appear (Figure 5B). The intensity of the new family of bands increases with the content of ethanol, and in 30% EtOH, the positive band disappears (Figure 5C). This behavior suggests that proflavine can interact with poly(dA-dT)·poly(dA-dT) according to two different binding modes, the first one prevailing in water and the second one being largely favored in the presence of EtOH. The behavior of the visible bands, corresponding to the CD induced by the binding of proflavine to the polymer,<sup>29</sup> also plays in favor of a change of binding modes. Actually, the negative band is barely observable in water (Figure 5A) but, in 10% EtOH this band is well formed, reaching its maximal extension in 30% EtOH. At the same time the positive band, associated with intercalation, has disappeared.

**Poly(dG-dC)·poly(dG-dC)/PR.** The evolution of the CD spectra of poly(dG-dC)·poly(dG-dC)/PR induced by addition of PR is rather similar to that of poly(dA-dT)·poly(dA-dT)/PR with the exception of the spectra recorded in the UV region for 30% EtOH (Figure 5C,F). The CD behavior also shows that two modes of binding are operative, the first one prevailing in water (Figure 5D), the second one being dominant in 30% EtOH (Figure 5F). The ability of EtOH and proflavine to modulate the occurrence of the two binding modes is better represented by the plots of Figure S7 of the Supporting Information, where the dependence of  $[\theta]$  at 425 nm on the  $C_D/C_P$  ratio is represented. Concerning poly(dA-dT)·poly(dA-dT), the change of binding mode occurs when the ethanol percentage becomes

**TABLE 2: Thermodynamic Parameters Corresponding to the Poly(dA-dT)·poly(dA-dT)/PR System Determined from the Melting Profiles at  $\lambda = 260$  nm,  $I = 0.1$  M (NaCl), pH = 7.0**

% (v/v) EtOH	$C_D/C_P$	$T_m$ (°C)	$\Delta H_{\text{vH}}^\circ$ (kcal mol <sup>-1</sup> )	$\Delta S_{\text{vH}}^\circ$ (cal mol <sup>-1</sup> K <sup>-1</sup> )	$\Delta G^\circ$ (kcal mol <sup>-1</sup> )	% hyperchromism [( $A_S - A_D$ )/ $A_S$ ] × 100 <sup>a</sup>
0	0.00	59.9	321	944	7.03	34
	0.11	62.0	316	920	7.11	32
	0.21	62.5	198	571	6.76	29
	0.32	63.2	174	499	6.51	24
	0.53	64.4	158	448	6.58	18
	1.07	66.6	133	371	6.61	15
	2.00	69.8	82	218	6.74	8
10	0.00	56.1	387	1155	6.92	36
	0.09	56.8	334	992	6.89	33
	0.18	57.4	299	885	6.68	28
	0.31	58.2	287	846	6.62	24
	0.49	59.1	301	885	6.79	19
	0.71	60.1	248	723	6.57	17
	0.98	61.0	252	734	6.58	14
	1.43	62.8	123	348	6.64	13
	1.92	63.6	130	367	6.50	9
20	0.00	50.5	121	345	8.78	30
	0.12	50.9	117	335	8.80	23
	0.24	51.1	111	316	8.88	18
	0.42	51.4	102	286	9.00	14
	0.66	52.1	110	312	8.67	10
	0.96	52.4	102	286	9.18	10
	1.33	53.0	127	363	8.89	7
	1.93	54.2	60	153	9.86	9
	0.00	46.4	180	542	6.39	36
30	0.13	46.6	177	533	6.42	24
	0.26	46.6	176	529	6.52	17
	0.45	46.9	176	529	6.49	12
	0.71	47.2	176	529	6.40	9
	1.03	47.4	190	574	6.52	7
	1.42	47.7	195	586	6.47	5
	1.98	48.4	114	334	6.68	7
40	0.00	42.6	155	472	6.23	28
	0.11	43.2	164	499	6.05	18
	0.23	43.0	180	548	6.35	14
	0.39	42.9	166	505	6.36	10
	0.62	43.5	183	558	6.18	7
	0.90	42.8	186	569	6.57	5
	1.24	44.5	120	357	6.63	6
	1.80	43.4	121	362	6.54	5

<sup>a</sup>  $A_D$  and  $A_S$  are the absorbance of the double helix and the single strand, respectively.

**TABLE 3: Enthalpy–Entropy Compensation Parameters at Different Percent EtOH for the poly(dA-dT)·poly(dA-dT)/PR System**

% EtOH	$a$ (K)	$b$ (kcal mol <sup>-1</sup> )	entropic term (cal mol <sup>-1</sup> K <sup>-1</sup> ) <sup>a</sup>
0	331	9.5	28.8
10	327	10.3	31.7
20	317	11.3	35.8
30	319	7.4	23.2
40	314	7.4	23.4

<sup>a</sup> Entropic term =  $b/a$ .

higher than 15% and for poly(dG-dC)·poly(dG-dC) the change is clearly observed only in 30% EtOH.

**Viscometric Measurements.** The plots of  $(\eta/\eta_0)^{1/3}$  vs  $C_D/C_P$  (Figure 6) show two linear tracts. For small  $C_D/C_P$  ratios the steep increase of  $(\eta/\eta_0)^{1/3}$  indicates intercalative binding. The reduction of slope observed for higher  $C_D/C_P$  values is suggestive of the onset of a binding mode that scarcely affects the contour length of DNA. According to Leszczynski et al.<sup>30</sup> the intersection of the two branches corresponds to a critical  $C_D/C_P$  ratio,  $r_{s,i}$ , related by eq 7 to the extent of unwinding,  $\Phi_i$ , induced into DNA by the binding process.<sup>31</sup>

$$\Phi_i r_{s,i} = \text{const} \quad (7)$$

The values of  $r_{s,i}$  obtained from Figure 6 are reported in Table 4, whereas the unwinding parameter for the DNA/PR system in water is known ( $\Phi_0 = 17^\circ$ ).<sup>32</sup> This value and that of  $r_{s,0}$  in water (Table 4) yield  $\text{const} = 5.95$ . By applying eq 7, we obtain the values of  $\Phi_i$  for the different EtOH/water mixtures that are collected in Table 4. Diminution of the unwinding angle,  $\Phi_i$ , with increase of % EtOH is in good agreement with a reduced content of intercalated proflavine.

**Kinetics.** The kinetic experiments have been performed by displacing the equilibrium by the  $T$ -jump method. Concerning the poly(dG-dC)·poly(dG-dC)/PR system, the relaxation curves are monoexponential (Figure S8 of the Supporting Information) and the dependence of  $1/\tau$  on the reactant concentration is linear (Figure 7) according to eq 8, where  $k_f$  and  $k_d$  represent respectively the forward and backward rate constants of the apparent reaction (2).

$$1/\tau = k_f([P] + [D]) + k_d \quad (8)$$

The values of  $k_f$  and  $k_d$ , obtained from plots as that of Figure 7 are reported in Table 5 together with their ratio  $k_f/k_d$ , which corresponds to the equilibrium constant,  $K$ , of reaction 2. Note that the kinetic method allows us to evaluate  $K$  in 30% EtOH,

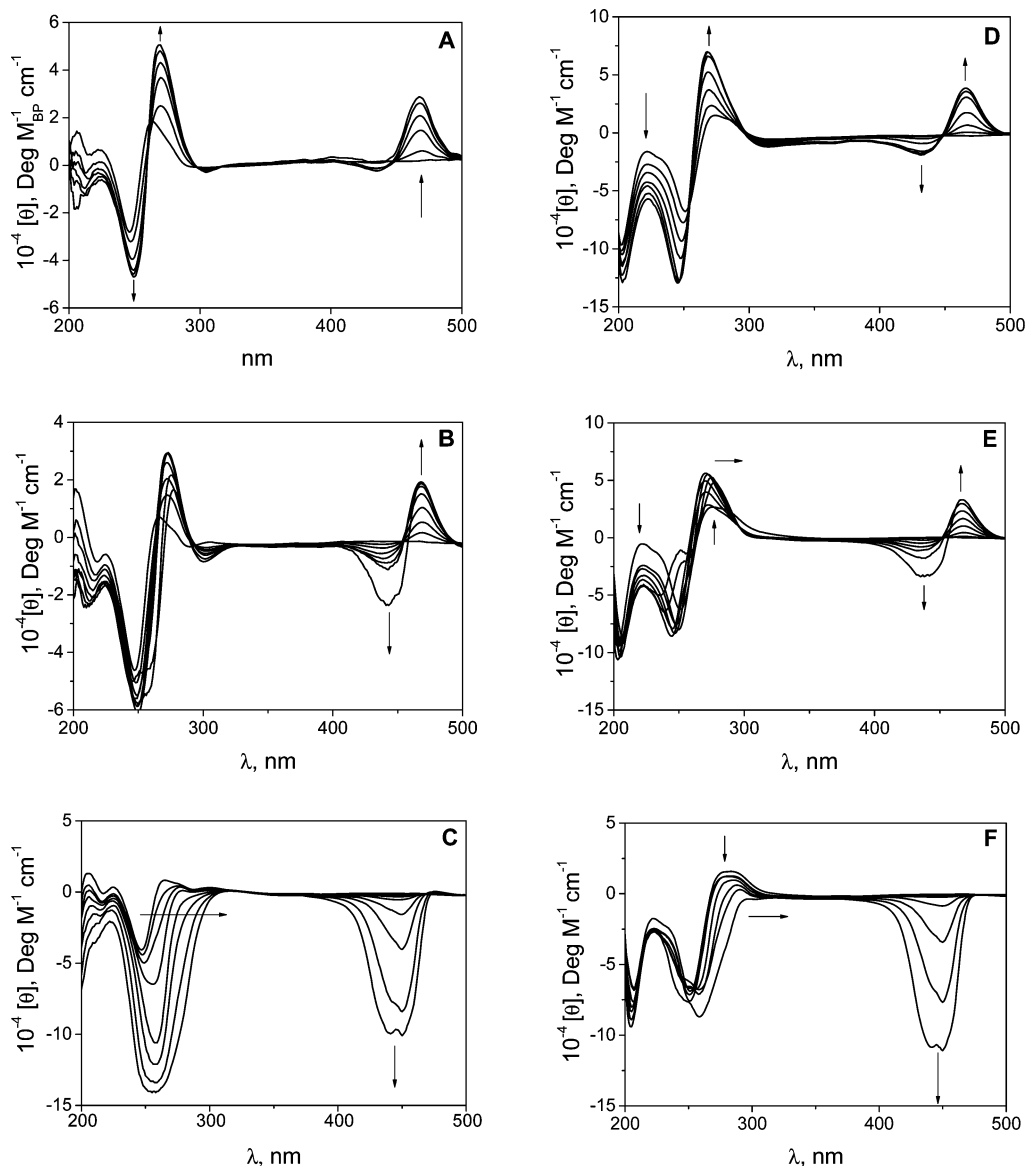


**Figure 5.** CD spectra of DNA/PR systems in different ethanol/water mixtures. Poly(dA-dT)•poly(dA-dT): (A) 0, (B) 10, and (C) 30% EtOH. Poly(dG-dC)•poly(dG-dC): (D) 0, (E) 10, and (F) 30% EtOH.  $C_D/C_P = 0, 0.15, 0.30, 0.50, 0.75, 1.00, 1.50, 2.00$  (arrows' sense).  $C_P = 1.5 \times 10^{-5}$  M,  $I = 0.1$  M (NaCl), pH = 7.0,  $T = 25$  °C.

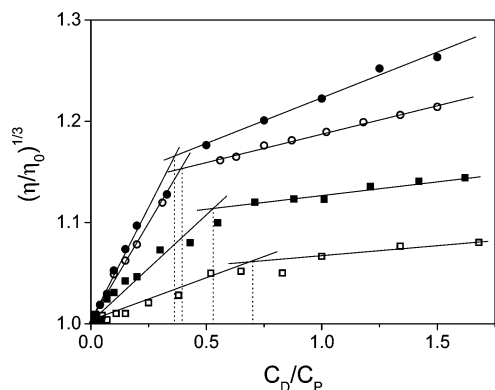


**Figure 6.** Plots of  $(\eta/\eta_0)^{1/3}$  for the CT-DNA/PR system as a function of the  $C_D/C_P$  ratio in different water/ethanol mixtures: (●) 0, (○) 10, (■) 20, (□) 30% EtOH.  $C_P = 2.20 \times 10^{-4}$  M,  $I = 0.1$  M (NaCl), pH = 7.0,  $T = 25$  °C.

while static titrations could not provide a reliable value of such a constant because of the too small signal variation at high ethanol content.

**TABLE 4: Values of  $r_{s,i}$  and  $\Phi_i$  Parameters at Different Percent EtOH for the CT-DNA/PR System**

% EtOH	$r_{s,i}$	$\Phi_i$
0	0.35	17.00
10	0.41	14.52
20	0.48	12.29
30	0.59	10.16

The poly(dA-dT)•poly(dA-dT)/proflavine system displays a more complex behavior. In 0% EtOH the relaxation curves are almost monoexponential (Figure 8A), although small deviations from monoexponential behavior could be observed at the highest values of  $C_D/C_P$ . Such deviations suggest that an excess of PR favors the change of binding mode in pure water, as also indicated by the loss of the isosbestic point induced by increase of the  $C_D/C_P$  ratio (Figure 1A). In 10% EtOH the kinetics are clearly biphasic, as shown by the biexponential fit to the experimental curve (Figure 8B). In 25% EtOH the system displays again an almost monophasic behavior (Figure 8C).

The reaction parameters are much lower than expected for a diffusion controlled reaction. This finding can be rationalized

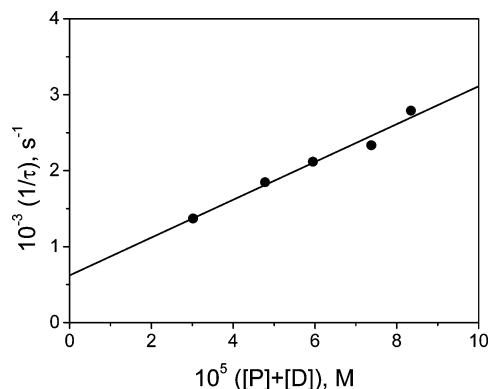


**Figure 7.** Dependence of the reciprocal relaxation time on the reactants concentration for the poly(dG-dC)•poly(dG-dC)/PR system in 10% EtOH.  $I = 0.1$  M (NaCl), pH = 7.0,  $T = 25$  °C.

**TABLE 5: Reaction Parameters for the Poly(dG-dC)•poly(dG-dC)/PR System at Different Percent EtOH ( $I = 0.1$  M (NaCl), pH = 7.0,  $T = 25$  °C)**

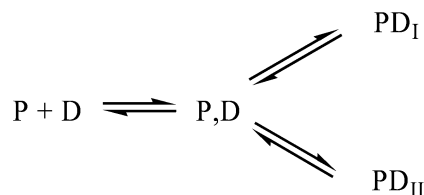
% EtOH (v/v)	$10^{-7}k_f$ (s $^{-1}$ •M $^{-1}$ )	$10^{-2}k_d$ (s $^{-1}$ )	$10^{-4}K$ (M $^{-1}$ ) <sup>a</sup>	$10^{-4}K$ (M $^{-1}$ ) <sup>b</sup>
0	4.3	6.8	6.3	6.1
5	5.3	5.7	9.3	10.3
10	2.5	6.2	4.0	5.0
15	2.4	6.0	3.9	3.9
20	1.1	13	0.9	1.0
25	2.1	14	1.6	0.86
30	1.4	15	1.0	

<sup>a</sup> Evaluated as  $k_f/k_d$ . <sup>b</sup> Evaluated from static titrations.

by assuming the diffusion controlled formation of a precursor complex that evolves to the final forms in subsequent, rate determining, steps.

The behavior of the two investigated systems can be rationalized by assuming the reaction in Scheme 1 where P,D is the precursor complex, while PD<sub>I</sub> and PD<sub>II</sub> are final complexes that differ for the position of proflavine bound to DNA. The

#### SCHEME 1



#### SCHEME 2



behavior of the poly(dA-dT)•poly(dA-dT)/PR system indicates that in water PD<sub>I</sub> is prevailing, in 30% EtOH the dominant species is PD<sub>II</sub> at any dye concentration, while at intermediate EtOH levels both complexes are present in the solution. The poly(dG-dC)•poly(dG-dC)/PR system displays a more sudden change of binding mode.

The branched mechanism depicted in Scheme 1 could be replaced by the kinetically indistinguishable series mechanism represented by Scheme 2, which has been favored by various authors.<sup>4,6,33</sup> Why scheme 1 should be preferred will be discussed below.

#### Discussion

The dependence of the equilibrium constants,  $K$ , displays a maximum at 10% EtOH in the case of the A-T/PR and 5% in the case of the G-C/PR system (Table 1). Such a trend inversion could result from a combination of electrostatic and hydrophobic forces that operate in opposite directions. At low EtOH contents the weakening of the hydrophobic forces is not sufficient to overcome the favorable dielectric constant effect, but when the EtOH level exceeds the above quoted limits, the hydrophobic forces start to prevail and the affinity decreases. Also, it should be noted that the EtOH/H<sub>2</sub>O mixtures show the maximum hydration capacity at about 10% EtOH.<sup>34</sup> This feature, denoted as “hydrophobic hydration” can enhance the affinity of the dye for DNA as it favors the stacking interaction.<sup>35</sup>

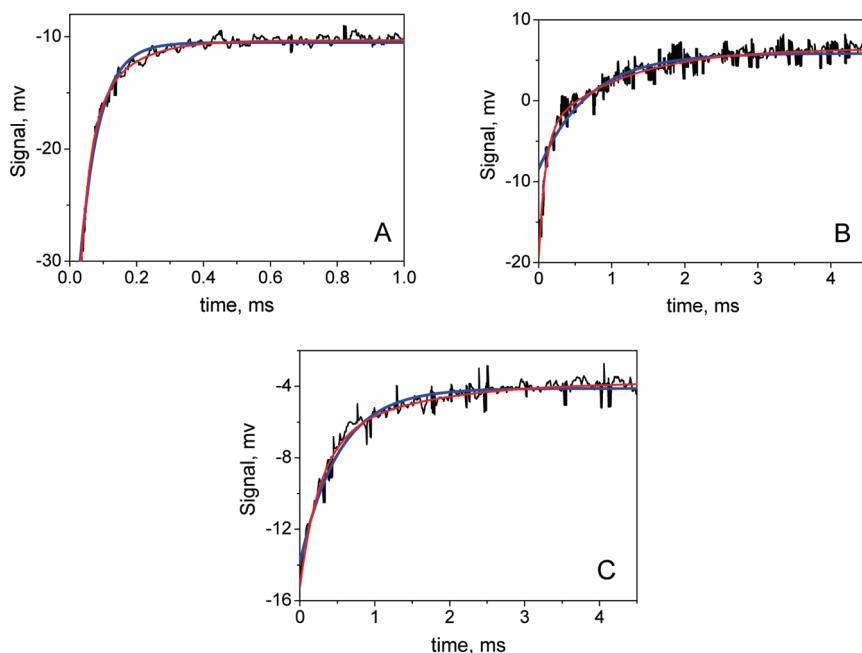


**Figure 8.** T-jump relaxation curve for the poly(dA-dT)•poly(dA-dT)/PR system in 0% (A), 15% (B), and 25% (C) EtOH.  $C_D = 7.6 \times 10^{-6}$  M,  $I = 0.1$  M (NaCl), pH = 7.0,  $T = 25$  °C,  $\lambda_{exc} = 455$  nm, (A)  $C_P = 1.00 \times 10^{-4}$  M, (B)  $C_P = 7.60 \times 10^{-6}$  M, (C)  $C_P = 2.28 \times 10^{-5}$  M. The continuous lines have been calculated according to a monoexponential (blue) or biexponential (red) data fit.



The lack of a well-defined isosbestic point in the visible spectra of the poly(dA-dT)•poly(dA-dT)/PR system suggests that more than a single complex could be formed during titration. Moreover, the increase of the site size induced by ethanol addition (Table 1) could reveal a change in the binding mode from prevailing intercalation in water to surface binding at high EtOH content.

The results of the melting experiments summarized in Figure 4 show that the  $T_m$  values decrease by increasing the EtOH content, corresponding to a destabilization of the double-stranded structure. In contrast, the increase of the dye concentration results in a reinforcement of the duplex structure. The last effect is more and more evident as the EtOH level tends to zero. Actually, in 0% EtOH the increase of proflavine concentration results first in a rather steep increase of  $T_m$ , which becomes less and less pronounced as the  $C_D/C_P$  level is raised, suggesting that a class of sites different from the intercalative ones starts to be filled at higher  $C_D/C_P$  values. In 40% ethanol, the increase of  $T_m$  is much softer, being less than 1 deg for the entire range of  $C_D/C_P$  values investigated, revealing that, under these circumstances, nonintercalative binding is dominant even at low  $C_D/C_P$  values. The van't Hoff melting enthalpy,  $\Delta H^\circ_{\text{vH}}$ , diminishes by raising the dye content, in contrast with the increasing trend of  $T_m$ . Inspection of Table 2 shows that at the lowest levels of EtOH an increase of proflavine results in a lowering of  $\Delta H^\circ_{\text{vH}}$ . An explanation of this observation can be provided if one considers that the measured thermodynamic properties in the presence of dye result from a combination of the thermodynamic properties of three processes, i.e., dissociation of on-slot dye from the polymer, dissociation of off-slot dye from the polymer, and double strand dissociation. Increase of dye content favors formation of the off-slot bound form, but this can dissociate from DNA more easily compared to the on-slot bound form, so that the heat required for the overall melting process is reduced. At the highest EtOH levels, the melting temperature is lower since the off-slot complex is prevailing over the entire range of  $C_D/C_P$  investigated; moreover, it is independent of the  $C_D/C_P$  values since the intercalation process and, by consequence, the corresponding thermal effect have been suppressed.

The obtained results can be interpreted in a quantitative way on the basis of the general thermodynamic model proposed by Starikov and Nordén.<sup>28</sup> Concerning the melting process of DNA/PR, it should be noted that this system is constituted by coupled reactions: the binding of the ligand to strands and strand dissociation. Changing the amount of ligand bound causes a shift of the energetics of the system in some way similar to the modification introduced by ligands of different but congener structure.<sup>36–38</sup> Such a shift can induce significant changes in both  $\Delta H$  and  $\Delta S$  of the melting process.<sup>39</sup> These circumstances could be suitable for the observation of the enthalpy–entropy compensation (EEC). Starikov and Nordén<sup>28</sup> have rationalized the EEC in terms of hidden but physically real factors implying a Carnot-cycle model in which microphase transitions (association/dissociation) play a key role. If the term  $b$  of the eq 6 is different from zero, as in the DNA/PR system here investigated, then the melting of the DNA/PR complex will involve a cyclic sequence of reversible phase transition, i.e., a closed thermodynamic cycle.

Valid enthalpy–entropy compensation phenomena were observed by Becker and Nordén for intercalation into DNA of 2–7 diazapyrene and its methylates cations<sup>36</sup> on one hand, and the piperazinylcarbonyloxyethyl derivative of anthracene and pyrene nonchiral<sup>37</sup> and chiral,<sup>38</sup> on the other hand. The piperazinylcarbonylalkoxyethyl ligands exhibit similar binding ge-

ometries, while the diazapyrenes show considerable chemical alterations. These differences reflect in the parameters of the  $\Delta H$  vs  $\Delta S$  plots. In particular, for both series the parameter  $b$  differs from zero; under these circumstances the Carnot cycle can be conceived as corresponding to a cyclic sequence of binding–debinding steps. Moreover, the first series displays a value  $T_{\text{comp}} = 361$  K higher than the working temperature ( $T = 298$  K), whereas the diazopyrene series shows  $T_{\text{comp}} = 282$  K (less than the working temperature). This result indicates that the Carnot cycles associated with the two systems operate in opposite directions.<sup>28</sup>

Table 3 shows that there is a clear nonmonotonicity in the “entropic term” ( $b/a$ ), which clearly shows the change of PR binding mode at 20% EtOH. Under these circumstances both binding modes, intercalation and surface binding, are operative and the entropy increase could be explained as due to the configurational entropy. Note that the entropic term in 40% EtOH is considerably lower than in 0% EtOH. This result could find an explanation in terms of different hydration of the DNA-PR complex, since such a high ethanol amount can destroy the hydration shell of the DNA–dye complex. Finally, the dependence of the “entropic term” reveals the importance of the hydrophobic effects in the system here studied.

The kinetic behavior of the poly(dG-dC)•poly(dG-dC) system is monophasic. The ratios of  $k_f/k_d$  calculated for different concentrations of EtOH yield values of the equilibrium constants in rather good agreement with the static values (Table 5). Table 5 also shows that the values of  $k_d$  are approximately constant ( $k_d = 6.2$  s<sup>−1</sup>) up to 15% EtOH, while between 20% and 30% EtOH a sudden increase of the dissociation rate is displayed ( $k_d = 14$  s<sup>−1</sup> as an average value). This behavior can indicate a change of binding mode, in agreement with the above-discussed results. At low EtOH content, where the on-slot complex is prevailing, the rate of dye dissociation is slower compared to that found at higher EtOH content, where the off-slot complex, more labile, becomes dominant.

Concerning poly(dA-dT)•poly(dA-dT), the biphasic kinetic behavior observed does not allow us to directly derive values of  $K$  to be compared with those obtained from static measurements.

Let us now discuss why, of the two reaction schemes presented above, we are inclined to reject scheme 2. Such a scheme reinforces the idea that PD<sub>II</sub> can only be formed at the expense of PD<sub>I</sub>. On the contrary, the CD spectra and the viscosity behavior in water and at low alcohol content suggest, as shown below, that Scheme 1 could represent more realistically the mechanism of site occupation.

The complex PD<sub>I</sub>, which is prevailing in 0% EtOH and at low values of the  $C_D/C_P$  ratio, presents all the characteristics of an intercalated (on-slot) complex. The values of the site size determined in 0% EtOH is less than 2 (Table 1). Also, the amplitude of the negative CD band at 430 nm, indicative of dye–dye interactions,<sup>29</sup> is small (Figure 5A,D), thus indicating that these interactions are in the minority compared to dye–base interactions. Moreover, electric dichroism and birefringence relaxation experiments, performed on the CT-DNA/PR system have shown that, at low degree of occupancy ( $r \approx C_D/C_P \leq 0.3$ ), all the bound dyes are oriented perpendicularly to the axis of the helix.<sup>40</sup> However, the presence of the negative CD band and the reduced ability of proflavine to unwind DNA ( $\Phi = 17^\circ$ ) compared with the unwinding ability of ethidium ( $\Phi = 26^\circ$ ) suggest that in PD<sub>I</sub> the proflavine could be not completely penetrated between base pairs. A fraction of the surface of the adjacent dye molecules stays outside the corresponding slot. Addition of ethanol induces a decrease of

the dye–base interactions (decrease of the amplitude of the positive band at 475 nm) to such an extent that in 30% EtOH the prevailing complex is PD<sub>II</sub>.

On the other hand, the elucidation of the nature of PD<sub>II</sub> is rather troublesome. The results of the present investigation show that PD<sub>II</sub> contains proflavine molecules located out of the DNA slots. These “off-slot” molecules can interact with the polymer by external stacking or groove binding. In the external stacking mode the molecules of PR are oriented perpendicular to the helix axis, forming long stacks stabilized by dye–dye interactions and, to a lesser extent, by dye–phosphate electrostatic interactions. This mode of interaction, which is operative in the ss-RNAs/PR system,<sup>41,42</sup> displays positive cooperativity that can be easily revealed by the thermodynamic and kinetic behavior of the system.<sup>41</sup> On the contrary, the systems here investigated do not exhibit any cooperative feature. One should mention, for this purpose, that EtOH tends to disrupt stacks of proflavine in aqueous solutions,<sup>43</sup> since it weakens the dye–dye interactions so important in the external stacking. On this basis, if PD<sub>II</sub> were an external stacked complex, its population would vanish at high EtOH levels, contrary to the experimental finding. Hence, we believe that in PD<sub>II</sub> the “off-slot” dye molecules are bound to the polymer groove. This kind of binding is characterized by a site size value higher than 2, as experimentally found. Further support to our conclusion is given by X-ray diffraction measurements on films of DNA/proflavine, which revealed that a change of humidity from 100% to 93% is able to induce the transfer of the dye from the intercalation sites to external sites.<sup>44</sup>

The CD spectra and viscosity trends highlight in the best way the evolution of the binding modes. Consider the poly(dA-dT)•poly(dA-dT)/PR system: in 10% EtOH both complexes are present (Figure 5B). The spectral sequence shows that, as the drug content is increased, the positive band (PD<sub>I</sub>) tends to saturation while the negative band (PD<sub>II</sub>) intensity continues to increase. This behavior reveals that PD<sub>II</sub> does not form at the expense of PD<sub>I</sub>. Actually, site occupation by proflavine first leads to formation of the intercalated complex and, once all intercalation sites have been filled, another class of sites (off-slot) starts to be occupied. This conclusion is confirmed by the viscometric experiments of Figure 7, which show that the filling of the sites corresponding to PD<sub>II</sub> starts after saturation of the intercalation sites.<sup>45,46</sup> On the basis of these results, one can exclude the reaction in Scheme 2, which requires the direct transfer of the ligand from PD<sub>I</sub> to PD<sub>II</sub>. The viscometric measurements also reveals that the intercalation process becomes less and less important as the EtOH level is raised, as indicated by the reduction of the slope of the first portion of the viscometric curve (Figure 7) and by the reduction of the unwinding angle (Table 4).

Table 1 shows that the site size does not reach the large values found in the case of classical groove binders. For instance, for the DNA/DAPI system a value of  $n$  of  $29 \pm 4$  was determined from spectrofluorometry experiments.<sup>47</sup> This fact suggests that proflavine could bind off-slot to DNA as an aggregate. Although the free drug concentration is below that of the self-aggregation limit,<sup>21</sup> it is not surprising that some PR molecules could bind to the hydrophobic groove surface in the form of aggregates. This thesis, already advanced,<sup>48</sup> is here supported by the splitting of the negative visible CD band associated with PD<sub>II</sub> which suggests that the ligand is bound to the groove, at least in part, as an aggregate (a dimer in the simplest case). The dimer peak, corresponding to the lower wavelength, increases on increasing the proflavine concentration. In agreement with the dimer destabilization effect induced by ethanol, in 10% EtOH the

[dimer]/[monomer] ratio is in favor of the dimer at the maximum value of added dye, whereas in 30% EtOH, at the same concentration of added proflavine, the dimer does not exceed the monomer.

## Conclusions

The effects induced by ethanol on the binding of proflavine to poly(dA-dT)•poly(dA-dT) and poly(dG-dC)•poly(dG-dC) have been investigated by a variety of techniques. The analysis of the data reveals that the increase of the alcohol content in the reaction medium produces a reduction of the dye affinity for DNA and also a change in the mode of interaction of proflavine from intercalative to surface binding. These results on one hand demonstrate that the electrostatic forces play a minor role in the binding process, and on the other hand point out the importance of the hydrophobic forces in driving the DNA–dye interaction toward the “on-slot” or the “off-slot” mode. Concerning poly(dG-dC)•poly(dG-dC), the transition between binding modes is rather abrupt, while for poly(dA-dT)•poly(dA-dT) the two bound forms coexist in solutions containing 5% to 25% EtOH. Interestingly, proflavine appears to be bound to the DNA surface in the form of an aggregate. The analysis of the enthalpy–entropy compensation of the DNA melting process at different EtOH contents provides a valuable method to observe the transition between the two proflavine binding modes.

**Acknowledgment.** We thank one of the referees for important suggestions concerning the enthalpy–entropy compensation phenomenon. Financial support by the Ministerio de Educación y Ciencia, Projects CTQ2006-14734/BQU and CTQ2009-13051/BQU, supported by FEDER, Junta de Castilla y León, Projects BU-013A-09 and GR257, Spain, are gratefully acknowledged.

**Supporting Information Available:** Absorbance variation at  $\lambda = 444$  nm as a function of proflavine concentration in different ethanol–water mixtures; binding isotherm corresponding to the poly(dA-dT)•poly(dA-dT)/PR system in 10% EtOH; analysis of the equilibria according to eq 3 for the poly(dA-dT)•poly(dA-dT)/PR and poly(dG-dC)•poly(dG-dC)/PR systems in 5% EtOH; Van't Hoff analysis of a melting curve of the poly(dA-dT)•poly(dA-dT)/PR system; DSC of the poly(dA-dT)•poly(dA-dT) system; plot of van't Hoff  $\Delta H$  vs  $\Delta S$  corresponding to the melting of poly(dA-dT)•poly(dA-dT) at different values of the  $C_D/C_P$  ratio; CD of DNA/PR systems vs  $C_D/C_P$  in different % EtOH;  $T$ -jump relaxation curve for the poly(dG-dC)•poly(dG-dC)/PR system in 5% EtOH. This material is available free of charge via the Internet at <http://pubs.acs.org>.

## References and Notes

- (1) Lerman, L. S. *J. Mol. Biol.* **1961**, *8*, 18–30.
- (2) Peacocke, A. R.; Skerrett, N. H., Jr. *Trans. Faraday Soc.* **1956**, *52*, 261–279.
- (3) Ramstein, J.; Ehrenberg, M.; Riegler, R. *Biochemistry* **1980**, *19*, 3938–3948.
- (4) Li, H. J.; Crothers, F. M. *J. Mol. Biol.* **1969**, *39*, 461–477.
- (5) Marcandalli, B.; Stange, G.; Holzwarth, J. F. *J. Chem. Soc., Faraday Trans. 1* **1988**, *84*, 2807–2819.
- (6) Biver, T.; Secco, F.; Tinè, M. R.; Venturini, M. *Arch. Biochem. Biophys.* **2003**, *418*, 63–70.
- (7) Marcandalli, B.; Winzek, C.; Holzwarth, J. F. *Ber. Bunsen-Ges. Phys. Chem.* **1984**, *88*, 368–374.
- (8) Ramstein, J.; Ehrenberg, M.; Riegler, R. *Biochemistry* **1980**, *19*, 3938–3948.
- (9) Chaires, J. B. *Biopolymers* **1985**, *24*, 403–419.
- (10) Baldini, G.; Varani, G. *Biopolymers* **1985**, *25*, 2187–2108.
- (11) Tanford, C. *The Hydrophobic effect*, 2nd ed.; Wiley: New York, 1980.

- (12) Reichmann, M. E.; Rice, S. A.; Thomas, C. A.; Doty, P. *J. Am. Chem. Soc.* **1954**, *76*, 3047–3053.
- (13) Schmechel, D. E. V.; Crothers, D. M. *Biopolymers* **1971**, *10* (3), 465–480.
- (14) Müller, W.; Crothers, D. M. *J. Mol. Biol.* **1968**, *35* (2), 251–290.
- (15) Schwarz, G.; Klose, S.; Balthasar, W. *Eur. J. Biochem.* **1970**, *12*, 454–467.
- (16) Carrier, V.; Savoie, R. *J. Sol. Chem.* **2000**, *29* (10), 1027–1038.
- (17) Cohen, G.; Eisenberg, H. *Biopolymers* **1969**, *8*, 45–55.
- (18) Biver, T.; De Biasi, A.; Secco, F.; Venturini, M.; Yarmoluk, S. *Biophys. J.* **2005**, *89*, 374–383.
- (19) Provencher, S. W. *J. Chem. Phys.* **1976**, *64*, 2772–2777.
- (20) Turner, D. H.; Flynn, G. W.; Lundberg, S. K.; Faller, L. D.; Sutin, N. *Nature* **1972**, *239*, 215–217.
- (21) Schwartz, G.; Klose, S.; Balthasar, W. *Eur. J. Biochem.* **1970**, *12*, 454–460.
- (22) Dewey, T. G.; Raymond, D. A.; Turner, D. H. *J. Am. Chem. Soc.* **1979**, *101*, 5822–5826.
- (23) McGhee, J. D.; von Hippel, P. H. *J. Mol. Biol.* **1974**, *86* (2), 469–489.
- (24) Jovin, T. M.; Striker, G. *Mol. Biol. Biochem. Biophys.* **1977**, *24*, 245–281.
- (25) Patel, D. J. *Acc. Chem. Res.* **1979**, *12*, 118–125.
- (26) Mergny, J. L.; Lacroix, L. *Oligonucleotides* **2003**, *13*, 515–537.
- (27) Duguid, J. G.; Bloomfield, V. A.; Benevides, J. M.; Thomas, G. J., Jr. *Biophys. J.* **1996**, *71*, 3350–3360.
- (28) Starikov, E. B.; Nordén, B. *J. Phys. Chem. B* **2007**, *111*, 14431–14435.
- (29) Fornasiero, D.; Kurucsev, T. *J. Phys. Chem.* **1981**, *85*, 613–618.
- (30) Leszczynski, T.; Dunski, H. *Zesz. Nauk. - Politech. Lodz., Chem. Spozyw. Biotechnol.* **2006**, *70*, 13–22.
- (31) Cantor, C. R.; Schimmel, P. R. *Biophysical Chemistry*; W. H. Freeman: San Francisco, 1985.
- (32) Graves, D. E.; Velea, L. M. *Curr. Org. Chem.* **2000**, *4*, 915–929.
- (33) Wakelin, L. P. G.; Waring, M. J. *Biopolymers* **1980**, *144*, 183–214.
- (34) Coccia, A.; Indovina, P. L.; Podo, F.; Viti, V. *Chem. Phys.* **1975**, *7*, 30–40.
- (35) García, B.; Ibeas, S.; Ruiz, R.; Leal, J. M.; Biver, T.; Boggioni, A.; Secco, F.; Venturini, M. *J. Phys. Chem. B* **2009**, *113*, 188–196.
- (36) Becker, H. C.; Nordén, B. *J. Am. Chem. Soc.* **1997**, *119*, 5798–5803.
- (37) Becker, H. C.; Nordén, B. *J. Am. Chem. Soc.* **1999**, *121*, 11947–11952.
- (38) Becker, H. C.; Nordén, B. *J. Am. Chem. Soc.* **2000**, *122*, 8344–8349.
- (39) Eftink, M. E.; Anusiem, A. C.; Biltonen, R. L. *Biochemistry* **1983**, *22*, 3884–3896.
- (40) Leng, M.; Ramstein, J.; Deubel, V.; Drocourt, J. L. *Stud. Biophys.* **1973**, *40*, 83–90.
- (41) Biver, T.; Ciatto, C.; Secco, F.; Venturini, M. *Archiv. Biochem. Biophys.* **2006**, *452*, 93–101.
- (42) Dourlent, M.; Helene, C. *Eur. J. Biochem.* **1971**, *23*, 86–95.
- (43) Dewey, T. J.; Raymond, D. A.; Turner, D. H. *J. Am. Chem. Soc.* **1979**, *101*, 5822–5826.
- (44) Neville, D. M., Jr.; Davies, D. R. *J. Mol. Biol.* **1966**, *17*, 57–74.
- (45) Cohen, G.; Eisenberg, H. *Biopolymers* **1969**, *8*, 45–55.
- (46) Suh, D.; Chaires, J. B. *Bioorg. Med. Chem.* **1995**, *3*, 723–728.
- (47) Healy, E. F. *J. Chem. Educ.* **2007**, *84*, 1304–1307.
- (48) Armstrong, R. W.; Kurucsev, T.; Strauss, U. P. *J. Am. Chem. Soc.* **1970**, *92*, 3174–3181.

JP102801Z